

Original Article

Deep Learning Approach for Diagnosing Papulosquamous Disease

G. Nagarajan¹, Arun Raaza², Chetna Dayanand Achar³, M. Meena⁴

¹Electronics and Communication Engineering, VISTAS, Chennai, Tamil Nadu, India.

²Centre for Advanced Research & Development, VISTAS, Chennai, Tamil Nadu, India.

³MET Institute of Computer Science, Mumbai, Maharashtra, India.

⁴Electronics and Communication Engineering, VISTAS, Chennai, Tamil Nadu, India.

¹Corresponding Author : gothandam.nagarajan@gmail.com

Received: 20 June 2024

Revised: 06 February 2025

Accepted: 13 February 2025

Published: 28 March 2025

Abstract - The six papulosquamous skin diseases, including psoriasis, psoriatic arthritis, eczema, and dermatitis, can be difficult to diagnose and treat due to their similar clinical manifestations. Diseases of the skin can be caused by a combination of environmental and genetic factors, and their consequences can be devastating. Developing early and automatic skin disease predictions is essential to reduce the dermatologist's workload and enhance treatment outcomes. This study uses the Xiangya-Derma knowledge-based clinical image database in order to gain a greater understanding of skin diseases. A complex deep neural network is trained from the images in the dataset to extract the affected area adaptively. Numerous statistical characteristics are extracted and analyzed using the NDL method. The classifier uses a training procedure and a number of stacked "layers" to recognize skin disease indicators. The effectiveness of the Python-implemented system under discussion was evaluated using a variety of performance metrics. In this research, 70% of the data was used for training, 20% for testing, and 10% for validation.

Keywords - Papulosquamous, China's largest clinical image dataset, Adaptive optimized convoluted deep neural network, Neuroevolution deep learning.

1. Introduction

Skin disease [1-3] or infection affects skin soft tissues such as mucous membranes and loose connective tissues. Skin disease is the most common in daily life, affecting almost every age group. Skin disease has been classified into skin neoplasm and infection; thousands of skin diseases are described among these two groups. This disease affects people and has an impact on their psychosocial mobility. Skin disease creates complexity in people's lives in all aspects, such as work, interpersonal relationships, physical activity, social functioning, and mental health [4]. Few people can identify skin diseases without requiring any reference and consume drugs to treat their infections [5]. The wrong identification of skin disease causes serious health issues and creates an economic burden in high-low-income countries. Skin disease generally leads to plaques, scales, and skin lesion symptoms on the patient's skin, which causes disfigurement and long-term pain [6]. These skin damages cause mental problems, especially when the skin problem occurs on the face [7]. According to various studies, people who suffer from primary skin diseases like alopecia areata, psoriasis, and vitiligo [8]. Sometimes, the prolonged treatment of the skin disease and its recurrence in the same location or at different locations in the

human body cause depression. In traditional skin forecast approaches, patients self-diagnose the skin disease, and images are taken and sent to the vision recognition process. The images are affected by several computer vision techniques [9, 10] to identify skin diseases. Nevertheless, the vision computer community cannot fully process and identify the skin issue from the image. This disease has no characteristic spatial organization, resulting in challenges when forecasting dispersed skin diseases such as red eczema [11]. Furthermore, the system does not have many challenges, such as insufficient contrast between surrounding skin and lesion, inappropriate fuzzy boundary, and variegated colour of the inner lesion, which creates difficulty in recognizing skin disease [12].

By considering these concerns, the researchers use dermoscopic images to detect skin disease. The dermoscopic photos have minimum noise as they are recorded under unique lighting. Aside from this, there are a variety of sources, like mobiles, digital cameras, etc., that allow for taking images of skin to help conduct the clinical process. By nature, the classification of the skin disease task belongs to the fine-grained visual object detection problem. The skin disease may happen at any location of the body; hence, the region's



features are diverse, which creates challenges while performing self-diagnosis. The clinical process needs a lot of information, such as skin lesion pattern, duration, symptoms, location, colour, etc., causes more time to make the clinical decision. Moreover, the presence of huge amounts of data on the internet enhances the computing capability of skin disease diagnosis. In most of the studies, the skin images captured are processed using deep-learning methods [15] to provide highly accurate performance for a large dataset.

In particular, the convolution network played a vital role in efficiently processing radiology and pathological images in the medical sector. Although clinical image-related studies are not many, that adds complexity in predicting skin disease. Thus, the relative skin image data set is implemented to enhance this work's whole skin disease prediction process. The data set involves different regions of body images, particularly the region of the face.

The facial image area is extremely tiny compared to the entire body but needs tremendous computation and processing analysis to anticipate the precise skin disease. Due to the high noise levels, complexity, and variation in texture in skin lesion images used for segmentation, a pre-processing step was necessary to mitigate their negative effects [16]. Segmentation of skin lesions due to their irregular shapes, colours, and textures, as well as image artifacts such as hairs and air bubbles, is a challenging task [17]. Existing domain adaptation approaches for skin lesion classification had lower recognition accuracy than supervised models [18].

In this paper, Xiangya-Derma knowledge-based CHINA's largest clinical image dataset [16] is utilized to predict skin disease by considering the overall discussion. The dataset consists of Actinic Keratosis (AK), Seborrheic Keratosis (SK), Lupus Erythematosus (LE), Rosacea (ROS), Squamous Cell Carcinoma (SCC), and basal cell carcinoma (BCC) Disease-Related Images. Almost the dataset has 4394 images, of which 2656 are facial images. Among the six diseases, SCC, BCC, ROS, and LE disease often occur on the face. The SK and AK disease are converted to malignant when not treated in a specific period.

The collected images are processed by an adaptive optimized convolute deep neural network that successfully removes the noise and segments the skin-affected region. The neuroevolution deep learning method is then applied to the extracted data to analyze the many statistical features. This optimized technique successfully predicts the exact skin disease patterns from the previously extracted and trained templates. The introduced system was implemented using Python. The system's efficiency was evaluated using various metrics such as mean square error rate, mean absolute error rate, intersection-over-union, dice coefficient, accuracy, confusion matrix, precision, recall, f1-score, and Mathew correlation coefficient.

1.1. The Importance of the Study

The main goal of this study is to find a way to classify operations with high accuracy and low loss. This helps doctors make more accurate diagnoses and determine what kind of lesion a person has much faster. In these situations, doctors must go above and beyond to develop accurate prognoses. The end goal of any research endeavour is to get quantifiable data.

1.2. The Value of Research

Diseases of the skin also cause deaths worldwide. The frequency with which this occurs in human society is steadily rising. Preventing a skin infection from developing into a skin disease is of paramount importance. There will be 197,700 new cases of skin disease diagnosed in the United States in 2022; this number will include 97,920 cases of non-invasive illness and 99,780 cases of invasive disease. Reliable diagnosis of skin illnesses is complicated by a worldwide shortage of well-trained dermatologists. A clear representation of the disease in the dermoscopy image can be obtained using deep learning and AI-enabled image analysis technology. Systems based on deep learning can potentially improve disease detection in the field of medicine by reducing the number of false positives and increasing the accuracy of visual analysis.

1.3. Industry-Wide Technical Consequences

The accuracy of Deep Learning (DL) image analysis algorithms is generally agreed upon. These models have recently been shown to outperform several state-of-the-art models in various settings. In addition to improving performance and accuracy in disease detection, deep learning processes also help reduce the number of errors made. To put it another way, a model with this methodology can aid in the tough decisions that need to be made by surgeons.

1.4. Competence on a National, Economical, and Technological Scale

Deep learning-based methods are currently being used in the medical field for a wide range of disease diagnosis tasks. Preventing a skin infection from developing into a skin disease is of paramount importance.

2. Related Works

Li-sheng Wei et al. (2018) [19] describe the application of Deep Learning (DL) techniques to analyze clinical images for detecting malignant and benign cutaneous tumours. The convolution network is involved in the Asan dataset, Atlas site images, and MED-NODE dataset for predicting the 12 skin diseases. The training model validates the Asan, Edinburg, and Hallym datasets to predict intraepithelial basal cell carcinoma, melanoma disease, and squamous cell carcinoma. Sourav Kumar Patnaik et al. [20] Uses the texture features and image colour to find the specific type of skin disease. This system uses a support vector machine algorithm to predict psoriasis, dermatitis, and herpes. The skin images are examined based on the Grey-Level Co-Occurrence Matrix

(GLCM), which segments the skin disease-affected region. The extracted features are more useful and feasible while treating skin disease with maximum accuracy. Srinivasu et al. (2021) [21] describe how they used deep learning to predict the skin disorder. This system predicts skin diseases as accurately as possible by using the architecture of Inception Resnet V2, Inception V3, and MobileNet. This analysis uses 1000 images to do the feature extraction, training, and testing steps of the skin detection process. By using three methods, the new system meets the research goal of making predictions as accurate as possible.

Zhe. Wu et al. (2019) [22] use MobileNet V2 and a Long-Short-Term Memory Neural Network (LSTM) to make a system for classifying skin diseases. This work uses the HAM 10,000 skin image dataset to figure out the disease as quickly as possible. A gray-level co-occurrence matrix investigates the images to derive the features. The extracted features are analyzed by an introduced classifier that predicts the disease with 85% accuracy. Then, the introduced system minimizes computation time and manages robustness.

Tri-Cong Pham et al., 2020 [23] Classifies the face's skin disease using different Convolutional Neural Network (CNN) algorithms on clinical images. The images are collected from Xiangya-Derm China's largest dataset, which consists of 2656 images. The images are classified according to the CNN architecture and the transfer learning process. This process classifies the skin disease with 92.9% accuracy, 70.8% precision, and 77.0% recall value.

Belal Ahmad et al., 2020 [24] enhances the skin disease identification process according to a customized loss function with balanced mini-batch logic augmentation. This system aims to handle the class imbalance problem while classifying skin diseases. A new loss function is built during the analysis process by combining the balance mini-batch logic and the real-time augmentation algorithm. The designed system uses 24,530 images that consist of seven disease details. From the analysis, the system classifies the skin disease with 89.97% accuracy. Thus, the author introduced a system that resolves the slow learning issues by designing a new loss function using a combined approach.

B. Ahmad et al., 2020, p. 25 uses a deep convolution neural network and discriminative feature learning to classify skin diseases. This system aims to minimize the time-consuming, subjective, and handling human effort. The learning technique is applied to embedding the images into Euclidean space according to the Inception ResNet-V2 and ResNet152 models. After that, the L-2 distance is computed from embedded Euclidean space to extract the discriminate features. Finally, the classification is performed to retrieve the skin disease with maximum accuracy. Peng Tang et al., 2020 [26] uses progressive transfer learning and adversarial domain adaptation techniques to figure out skin disease. Initially, the

deep convolution network is applied for the pre-training process. Then, adaptation techniques like the adversarial learning approach are used to recognize the skin disease. This learning process helps to predict the cross-modality, cancer, and melanoma detection processes.

Jufeng Yang et al., 2020 [27] Uses global parts of CNN and the ensemble learning method to classify skin lesions. This study intends to minimize the intra- and inter-class variation while examining the skin lesion images. The introduced method uses fine-grained local and global context information to process the large volume of data with minimum computation time and high skin disease recognition accuracy. Anuj Kumar Singh et al., 2021 [28] Uses a Self-Paced, Balanced Learning Approach (SPBL) to make a system to find skin diseases in a clinical setting. This system uses the SD-260 and SD-198 dataset images to investigate skin disease.

The self-paced learning paradigm explores the image features and predicts the disease using each class's penalty weight assignment. Based on what different authors have said and how they have talked about skin disease, it has been decided that it can affect any body part. Most of the researchers use dermatology images, which are processed with the help of a deep-learning approach. The network has an effective way to learn, which will help researchers look into the huge amount of data with as little time and complexity as possible. In this work, effective and optimized deep learning techniques are introduced by considering their research opinions and ideas. This newly introduced technique improves the overall skin disease recognition process with a minimum misclassification rate.

3. Materials and Methods

3.1. Dataset Description

This study uses the Xiangya-Derm [https://www.medicalimageanalysis.com/data/skinia/Xiangya-Derm]. <http://airl.csu.edu.cn/xiangyaderm/> face image dataset, which consists of six skin diseases: Actinic Keratosis (AK), Seborrheic Keratosis (SK), Lupus Erythematosus (LE), Rosacea (ROS), Squamous Cell Carcinoma (SCC), and Basal Cell Carcinoma (BCC). This database is created according to skin disease. It has 47075 clinical images that show 541 skin diseases. These images were captured with the help of a digital camera and matched with medical and pathology histories. Central South University issues the developed database images for the Department of Dermatology. According to the discussion, the captured face skin disease image is illustrated in Figure 1, and details are described in Table 1.

According to Table 1, the dataset has 4394 images, of which 2656 are face images. The total images are divided into training (2,656) and testing (388) images. With the help of these images, an automatic computer-aided system is developed to predict skin disease. The gathered sample skin images are illustrated in Figure 1.

Table 1. Dataset description

Diseases	Number of Images	Face Images	Images Involved in Training	Images Involved in Testing
BCC	689	578	623	66
LE	1273	781	1188	85
AK	277	108	219	58
SCC	710	413	638	72
SK	1127	593	1075	52
ROS	318	183	263	55
Total	4394	2656	4006	388

Once the images are collected, they are processed using computer-aided techniques to predict the skin disease. The automatic system uses various steps such as image pre-processing, region segmentation, feature extraction, and classification. Every step played an important role in classifying skin diseases.

Region segmentation and feature extraction are crucial among these steps because the disease-affected region and neighbouring regions differ in only a few characteristics. Therefore, the disease-infected area should be recognized, leading to an increased overall rate of skin disease identification. The feature extraction step is more powerful

because it derives the disease-relevant statistical and texture features that reflect the disease information. According to the discussion, the overall working process of the skin disease detection process is illustrated in Figure 2.



Fig. 1 Sample skin disease images

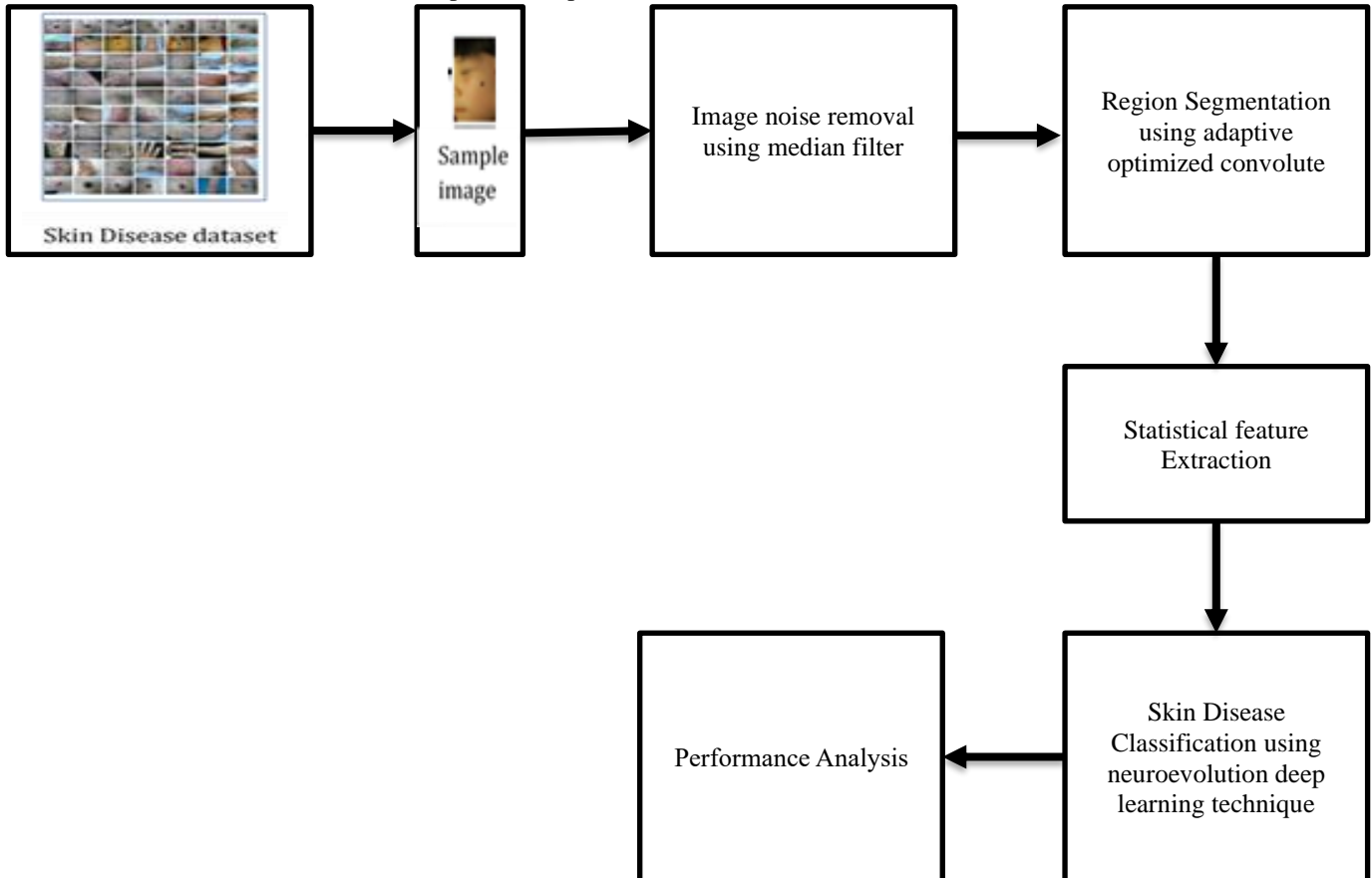


Fig. 2 Process flow of skin disease classification

3.2. Methodology Discussion

3.2.1. Skin Image Noise Removal Using the Pre-Processing Technique

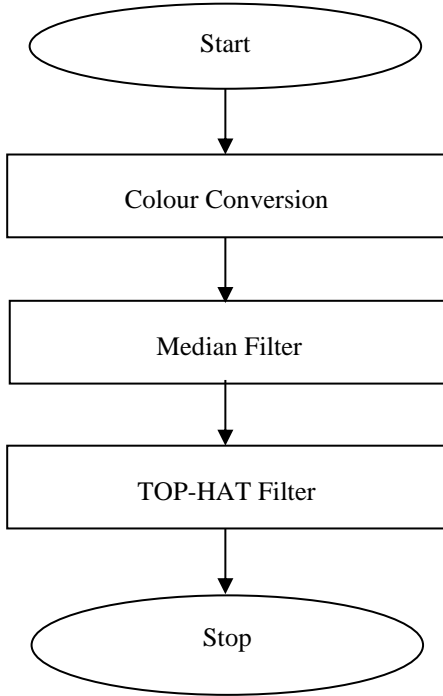


Fig. 3(a) Pre-processing stage flow

The entire pre-processing stage flow diagram has been shown in Figure 3(a). The first step of this work is to remove noise from captured facial skin images. The images are acquired in different aspects, which cause changes in image resolution and noise involvement in skin images. The noisy images affect the entire efficiency of skin disease classification. As a result, before segmenting the affected region, the image noise must be removed first. In this work, negative impacts and noise from the image were removed using median filtering. This technique identifies the irrelevant background details and removes the salt and pepper noise without affecting the image edge details. By computing the gray-pixel median value, it helps to smooth the image. Then the noise removal process is done by using Equation (1).

$$F'(x_0, y_0) = [sort_{(x,y) \in S} F(x, y)]_{(N+1)/2}, N \geq 0 \quad (1)$$

The median value is estimated from the neighbourhood collection S of image pixels (x, y) . The element of each pixel is analyzed continuously and sorted to compute the median value. Each grey value replaces the computed median value. After smoothing the image, it should be denoised to improve the quality of the image. The denoising process is done according to the neighbourhood sampling process. Consider image I , which is rotated at an angle, and the new weight and height of the image are obtained according to Equations (2(a) and 2(b)).

$$neww_{width} = 2 * \left(\left| \left(\frac{w}{2 * \cos \theta} \right) \right| + \left| \left(\frac{h}{2 * \sin \theta} \right) \right| \right) \quad (2a)$$

$$newh_{height} = 2 * \left(\left| \left(\frac{h}{2 * \cos \theta} \right) \right| + \left| \left(\frac{w}{2 * \sin \theta} \right) \right| \right) \quad (2b)$$

In Equations (2(a) and 2(b)), w and h are represented as the width and height of the image. The new and value is obtained by rotating the image by an angle from the old w and h values. The image coordinates are obtained using Equations (3(a) and 3(b)).

$$(x_0 - x_{r1}) = (x_1 - x_{r2}) * \cos \theta - (y_1 - y_{r2}) * \sin \theta \quad (3a)$$

$$(y_0 - y_{r1}) = (x_1 - x_{r2}) * \sin \theta - (y_1 - y_{r2}) * \cos \theta \quad (3b)$$

In the above Equations (3(a) and 3(b)), original coordinates are denoted as the image I central coordinates are (and the transformed coordinates are this sampling process transformation is performed using Euclidean geometry. Along with this, brightness pixels are derived to enhance the quality of the image, and neighbouring pixels are computed using distance measurements, which are mentioned in Equation (4).

$$d(p_{x,y}, b_{mn}) = \sqrt{(x - m)^2 + (y - n)^2} \quad (4)$$

The Euclidean distance $d(p_{x,y}, b_{mn})$ is defined as the medial axis transform of x and y coordinates $p_{x,y}$. To overcome the issues related to noise, the Top Hat filter was used in combination with the conventionally used median filter in this research work. According to the discussion, the noise-removed sample images are illustrated in Figure 3(b).

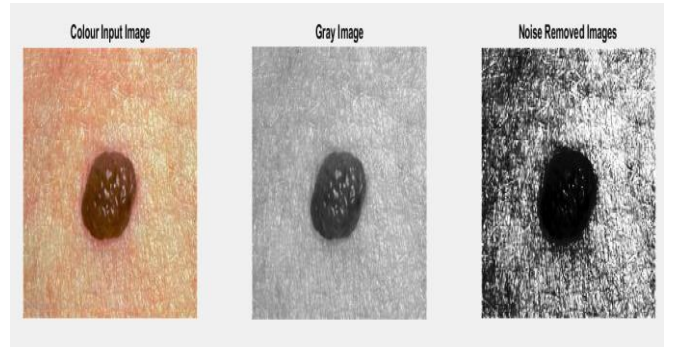


Fig. 3(b) Sample noise removed images

Once the image noise is removed, the affected region must be segmented to identify the skin disease.

3.2.2. Region Segmentation Using Adaptive Optimized Convolute Deep Neural Network

The second process is region segmentation, which is performed by applying adaptively optimized convolution deep neural networks. The convoluted deep neural network recognizes the affected region by using different layers. During this time, the network learning rate must be set before

training the model, which consumes more time. To overcome this issue, the adaptive optimization technique is applied in this work because it requires an initialized learning rate of 0.001. The defined learning rate is optimized and updated continuously by an adaptive method, which improves the overall training process. In this research work, to overcome the issues in segmentation, a hybrid algorithm of the Adadelta optimization technique with the convoluted network is used, causing an improvement in the overall performance of the skin region segmentation process. This optimization algorithm works based on the exponential moving average value of the squared delta. The delta value is obtained from the difference between the current weight and the newly updated weight. The computed delta value helps to replace the learning rate in the neural network function. The network weight value updating process is defined in Equation (5).

$$w_{t+1} = w_t - \frac{\sqrt{D_{t-1} + \epsilon}}{\sqrt{v_t + \epsilon}} \cdot \frac{\partial L}{\partial w_t} \quad (5)$$

Equation 5 defines the weight updating process that helps predict the new weight value and the affected skin region. As discussed above, the pre-processed skin images are processed by convoluted network layers such as convolution layers, fully connected layers, and an output layer.

The convoluted network detects the skin disease-affected region in terms of the pixel output estimation process. This up-sampling is performed via deconvolution because the convolution layer produces only the smaller output size. Because of this, the network employs the max-pooling process, and the results are smaller in size. Therefore, up-sampling is performed to get the large output size. Then, a full convolution layer is applied to investigate the detailed information involved in the image. The deep investigation gives in-depth knowledge, but most of the time, spatial information is missing. Hence, the analysis is further improved element-wise, and the fusing process is performed to get the exact output images. This fusion is done by using the ResNet50 architecture. ResNet50 is a residual neural network that is 50 layers deep. It can also be used as a backbone neural network for different computer vision tasks. It consists of four convolution blocks, named Stages 1, 2, 3, and 4, as shown in Figure 4. Each convolution block includes three convolution layers with sizes of (1 * 1), (3 * 3), and (1 * 1) and a different number of filters. After all the convolution blocks, in the last step, a fully connected layer is connected, and a prediction of skin disease class is performed. According to the above process, affected regions are identified, and the sample region's recognized images are illustrated in Figure 5.

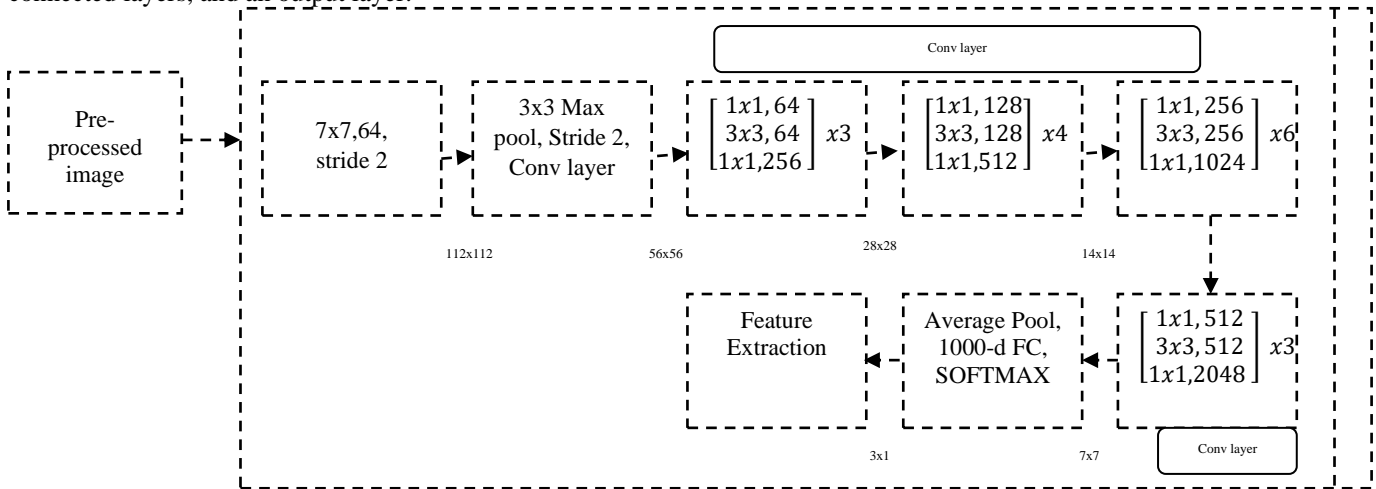


Fig. 4 ResNet50 architecture

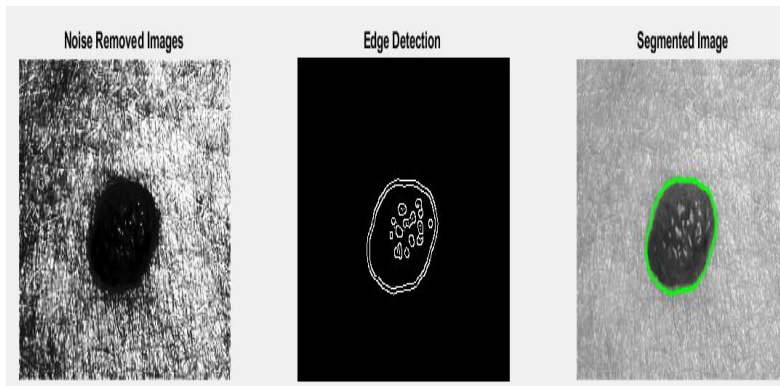


Fig. 5 Sample segmented region images

3.3. Feature Extraction

Once the affected region is derived, various texture and colour-related features are extracted [30, 31]. These extracted

features resemble those of skin diseases. The derived features are illustrated in Table 2. The extracted feature values differ from normal skin disease region-related features.

Table 2. Extracted features

	Positive	Predicted	Negative	
Positive	True Positive (TP) Correct objects		False Negative (FN) Missed objects	Recall = TP / (TP+FN) Accuracy = (TP+TN) / (TP+TN+FP+FN) F1 = 2 x Recall x Precision / (Recall + Precision)
Actual				
Negative	False Positive (FP) Extra objects		True Negative (TN) No objects	Specificity = TN / (TN+FP)
	Precision = TP / (TP+FP)		Negative predictive value = TN / (TN+TP)	

3.4. Skin Disease Classification

The last step of this work is skin disease classification, which is done by applying the neuroevolutionary deep learning technique. This algorithm is a subfield of artificial intelligence technique used to construct the network using evolutionary algorithms. The evolutionary approach recognizes skin disease according to the function of brain function by applying evolutionary algorithms. During this process, the network uses neuroevolution to consider the network to generate the network weight value, and the network topology is applied to evaluate the network weight value.

As discussed earlier, the network should train the features to make the classification process more effective. Here, the neuroevolution technique generates the network to train the features. Here, deep learning networks are utilized to perform this task. The network is working according to an artificial neural network inspired by biology. This network architecture uses several variations that consist of a grouping module layer (convolution and pooling) and a fully connected layer.

By considering these modules, the general architecture of this network for skin disease classification is illustrated in Figure 6. The proposed deep neural network model is utilized to classify skin lesions based on images obtained from dermoscopy. The deep neural network model has different convolution blocks consisting of convolution layers and max pooling layers. The original image size is 450 by 600 and resized to 28 by 28 by 3. The resized image is given to the first convolution block of the proposed deep neural network model. The first convolution block includes one convolutional layer and one max pool layer. The first convolution layer includes 32 filters of size (3 * 3) and a max pooling layer of size (2 * 2). The second convolution block has two convolutional layers

and one max pool layer. The filters of both the convolution layers are of size (3 * 3), with 16 and 32 filters, respectively, and the max pool layer is of size (2 * 2). The third convolutional block again consists of two convolutional layers and one max-pool layer. The filters of the third convolution layer are of size (3 * 3) with 16 and 32 filters, respectively, and the max pool layer is of size (2 * 2). After the third convolution block, the flattening layer flattens all features by converting feature space into a single feature vector.

In the last step, three dense layers are applied to classify the feature vector into seven skin disease classes. The block diagram of the proposed deep neural network model architecture is shown in Figure 6. In this work, no padding is used, and the default stride value is used. The default stride is (1,1). The default stride is 1, meaning that the filter will move one pixel to the right for each horizontal movement of the filter and one pixel down for each vertical movement of the filter.

Figure 6 depicts the elements of the proposed deep neural network used for research. The pre-processed and segmented images are given to the RESNET 50 network. RESNET 50 network was utilized because it's ideal for our research because of the number of images in the dataset. 4394 images were utilized for this research. The extracted features were obtained as output from the RESNET 50 network. 70% of the images were used to train the model. Neuroevolutionary Deep Learning (NDL) was used to do better optimization of the convolutional neural network during the backpropagation. The NDL algorithm provides better hyperparameter tuning and optimization, causing the intended increase in accuracy. Table 3 gives the various important design configuration parameters of the various elements of our proposed model.

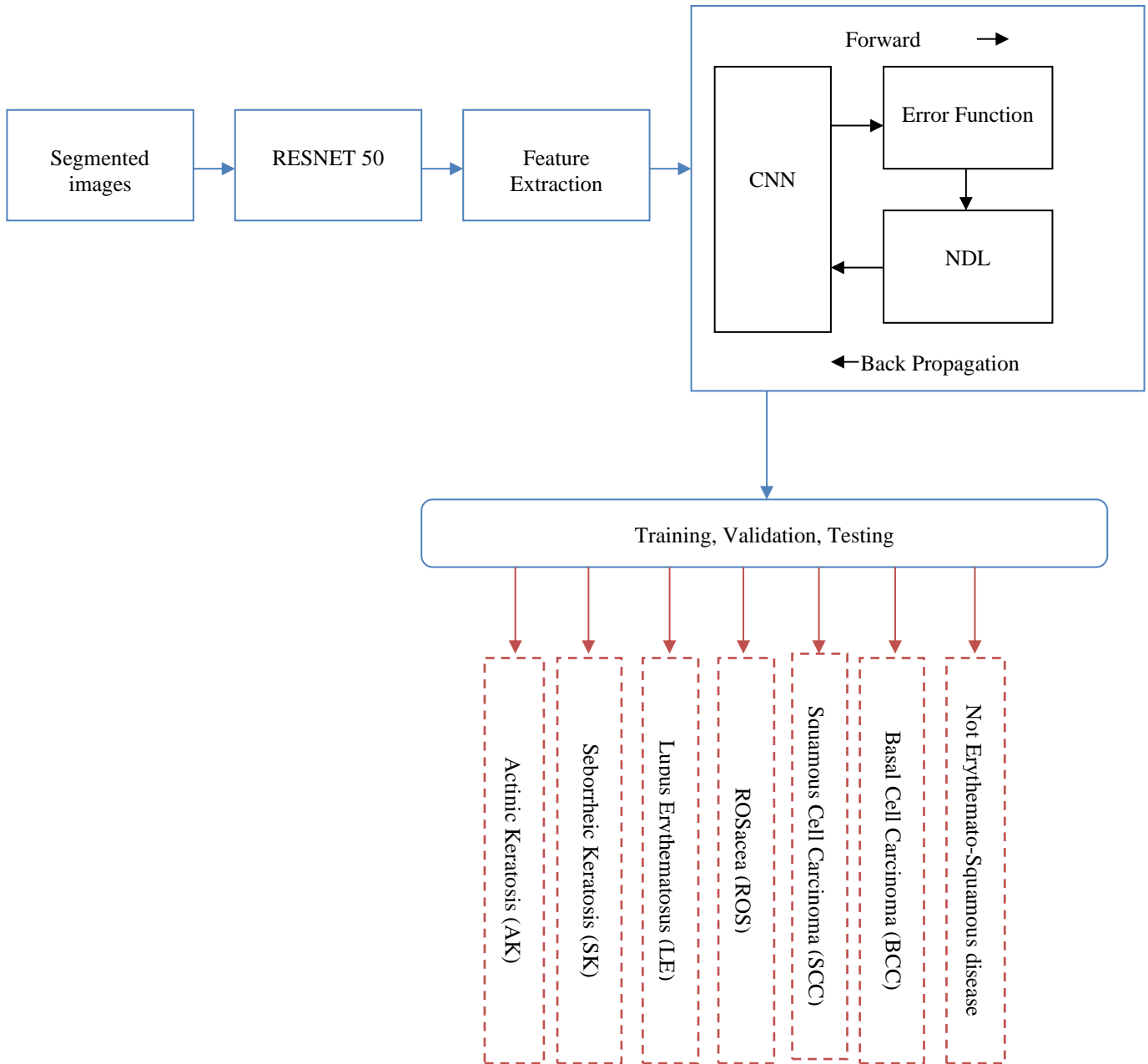


Fig. 6 NDL architecture

Table 3. The configuration information of the proposed model

Model	: Torch Vision, NDL
Base Learning Rate:	0.1
Learning Rate Policy:	Step-Wise (Reduced by a factor of 10 every 30/3 epochs)
Momentum	: 0.95
Weight Decay	: 0.0001
Cycle Length	: 10
PCT-Start	: 0.9
Batch Size	: 50

4. Results and Discussion

This section discusses the optimized deep neural network-based skin disease detection system. This process uses the Xiangya-Derma knowledge-based dataset, China’s largest clinical image dataset, for analyzing skin disease. The dataset consists of a large volume of skin disease images processed by applying the introduced technique. Before applying the deep learning technique, this work uses the median filter to eliminate noise and smooth the process. This process preserves the edge information that helps improve the exact region segmentation process. More than ever, the deep learning technique automatically derives the image features and patterns by applying the different layers. During this

process, adaptive optimization techniques are applied to improve the overall performance and reduce the complexity of extracting the affected region’s related characteristics. Further, the derived features are more useful for categorizing the skin disease with the highest rate. The dataset is split into three parts, such as training (70%), testing (20%), and validation (10%), by using stratified K-fold cross-validation [35, 36]. The data in the dataset were shuffled to ensure the obtained results were not false.

4.1. Stratified K-Fold Cross Validation

It is a way to get the most out of the data you have when training and testing a model. The algorithm is as follows:

- The data set is partitioned into k subsets (or folds) randomly.
- One subset is kept aside for validation, while the remaining subsets are used to train the model.
- To measure the prediction error, run the model on the hidden data.
- Go on until each k subset has been used as the test set.
- Determine the mean of the k observed discrepancies.
- The cross-validation error serves as a benchmark for the model’s performance.
- Stratified K-fold Cross-Validation (CV) is a reliable technique for determining a model’s precision.

4.2. System Analysis

Then, different metrics like the mean square error rate, mean absolute error rate, intersection-over-union, dice coefficient, accuracy, confusion matrix, precision, recall, F1-score, and Matthew Correlation Coefficient (MCC) were used to measure how well the system worked.

$$MAE = \frac{\sum_{i=1}^{no. of class} |Actual\ disease\ class_i - Predicted\ disease\ class_i|}{Actual\ disease\ class_i} \quad (6)$$

$$Mean\ Square\ Error, \quad MSE = \frac{\sum_{i=1}^n (Actual\ disease\ class_i - Predicted\ disease\ class_i)^2}{no. of class} \quad (7)$$

$$Accuracy = (TP + TN) / (TP + TN + FP + FN) * 100\% \quad (8)$$

$$precision = \frac{TP}{TP+FP} \quad (9)$$

$$Recall = \frac{TP}{TP+FN} \quad (10)$$

$$F1\ score = 2 \cdot \frac{precision \cdot recall}{precision + recall} \quad (11)$$

$$MCC = \frac{TP * TN - FP * FN}{\sqrt{(TP+FP)(TP+FN)(TN+FP)(TN+FN)}} \quad (12)$$

The above metrics are used to examine the performance of the newly introduced, optimized deep-learning neural network-based skin disease classification system. The discussed system is compared with existing research [17], Long-Short Term Memory neural network (LSTM) [20], and Self-Paced Balanced Learning approach (SPBL) [26-29]. According to the discussion, the obtained results for various classes and methods are illustrated in Table 4. As appeared in Table 4, the adaptive optimized deep learning technique attains a minimum error rate while classifying skin diseases of different classes.

This method ensures a 0.12 value for MAE and 0.1 for MSE metric. The obtained error rate values are minimal compared to existing methods such as DL (MAE-0.31, MSE-0.30), LSTM (MAE-0.22, MSE-0.21) and SPBL (MAE-0.18, MSE-0.181).

Not only the existing system, the introduced method ensures minimum error value on various types of skin diseases such as Actinic Keratosis (AK), Seborrheic Keratosis (SK), Lupus Erythematosus (LE), Rosacea (ROS), Squamous Cell Carcinoma (SCC), and Basal Cell Carcinoma (BCC). The obtained results plotted for comparison are shown in Figure 7.

Figure 7 clearly illustrates that the introduced system has a minimum error value compared to other methods. The introduced method starts with the noise removal process, in which the filtering technique eliminates the noise in each pixel according to the window moving and median value replacement processes. In addition to this, a new image orientation value is obtained according to the angle. This process eliminates the noise from the image without affecting the edge details.

Table 4. MAE and MSE

Method	Metric	BCC	LE	SK	ROS	AK	SCC	Average
DL [17]	MAE	0.345	0.317	0.287	0.2873	0.302	0.367	0.31
	MSE	0.310	0.318	0.293	0.263	0.312	0.323	0.30
LSTM [20]	MAE	0.268	0.246	0.215	0.21	0.18	0.23	0.22
	MSE	0.22	0.210	0.203	0.198	0.197	0.258	0.21
SPBL [26]	MAE	0.218	0.189	0.179	0.183	0.168	0.201	0.18
	MSE	0.201	0.180	0.184	0.178	0.158	0.187	0.181
Proposed	MAE	0.123	0.13	0.103	0.135	0.12	0.12	0.12
	MSE	0.109	0.103	0.101	0.11	0.09	0.087	0.1

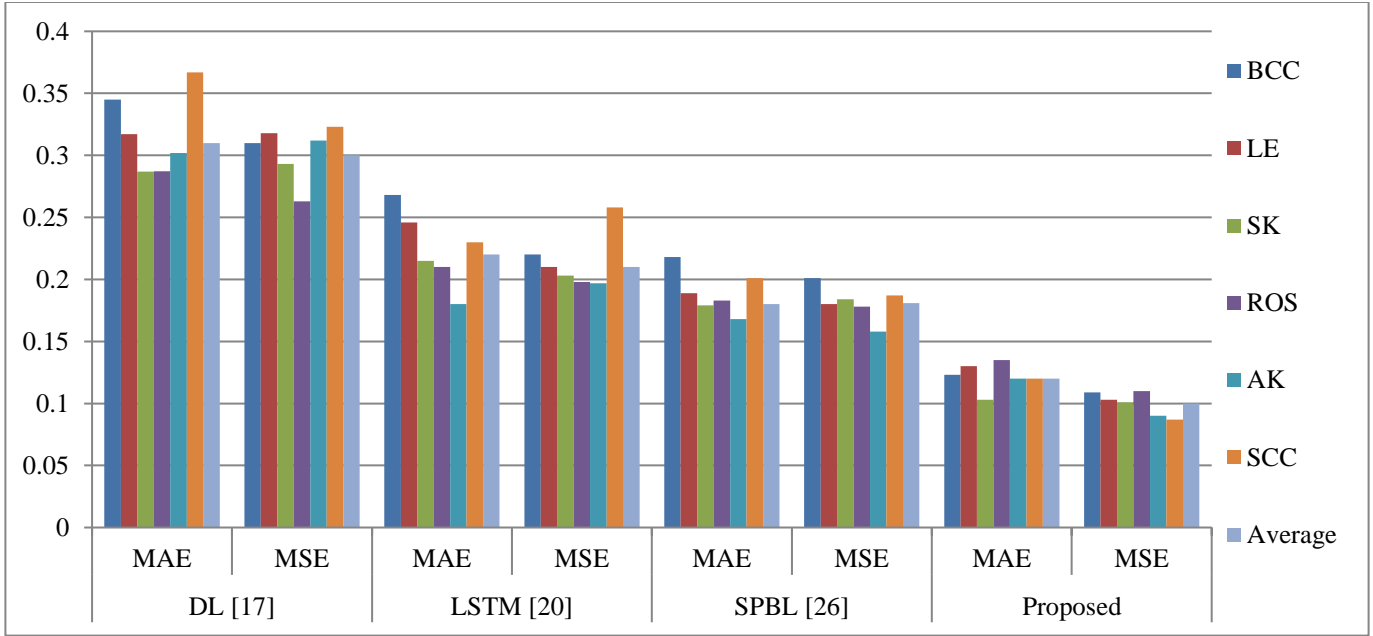


Fig. 7 Error rate

Table 5. Segmentation efficiency

Method	Metric	BCC	LE	SK	ROS	AK	SCC	Average
DL [17]	IoU	94.57	94.87	95.1	94.98	95.17	94.89	94.93
	DC	95.98	95.87	95.6	95.13	95.38	95.62	95.5967
	ACC	95.275	95.37	95.35	95.055	95.275	95.255	95.2633
LSTM [20]	IoU	95.289	95.87	95.92	95.92	95.97	96.29	95.8765
	DC	96.28	96.48	96.82	96.29	96.74	96.89	96.5833
	ACC	95.7845	96.175	96.37	96.105	96.355	96.59	96.2299
SPBL [26]	IoU	97.289	97.48	96.98	97.48	97.58	97.82	97.4382
	DC	97.83	97.85	97.97	98.03	97.98	98.23	97.9817
	ACC	97.5595	97.665	97.475	97.755	97.78	98.025	97.7099
Proposed	IoU	98.98	98.94	99.3	99.03	99.13	99.034	99.069
	DC	99.28	98.34	98.67	99.48	98.89	99.01	98.945
	ACC	99.13	98.64	98.985	99.255	99.01	99.022	99.007

This gives an effective platform to continue the further analysis of the skin disease recognition process. In addition to this, the method updates the network process according to the adaptive optimization technique related to weight values $w_{t+1} = w_t - \frac{\sqrt{D_{t-1} + \epsilon}}{\sqrt{v_t + \epsilon}} \cdot \frac{\partial L}{\partial w_t}$ that minimize deviation while segmenting the disease-affected region and identifying normal regions.

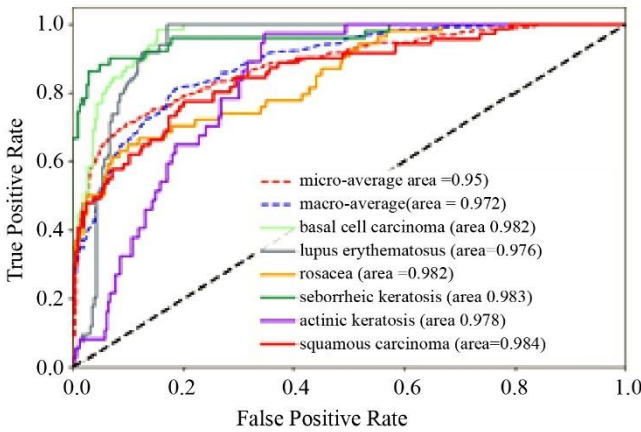
More than that, the minimum error value shows that the system used to recognize the skin disease is as accurate as possible. Further, the segmentation region's effectiveness is illustrated using the Intersection-Over-Union (IoU), Dice Coefficient (DC), and Accuracy (ACC) metrics. Then, the obtained results are illustrated in Table 5. As appeared in Table 5, an adaptive optimized deep learning technique ensures high accuracy while segmenting the skin disease-affected region. This method ensures 99.069% for IoU, 98.94% for DC, and 99.00% for the ACC metric. The obtained

segmentation efficiency value is the maximum when compared to existing methods such as DL (IoU-94.93%, DC-95.59%, and Acc-95.26%), LSTM (IoU-95.87%, DC-96.58%, and Acc-96.22%), and SPBL (IoU-97.43%, DC-97.98%, and Acc-97.70%).

Due to the effective utilization of the convolution layer in the deep learning network, it helps identify the exact disease-affected region. During this process, the method investigates each pixel, which helps to understand the characteristics of each pixel. Then, the method uses the ResNet50 model with an adaptively optimized learning rate. The model categorizes each pixel to its respective class with a minimum error rate and maximum segmentation accuracy rate. Accurately predicting the affected region improves the overall classification rate of skin diseases. However, the effectiveness of the introduced system was determined using the confusion matrix shown in Figure 8.

		Index of predicted class					
Index of true class	0.97	0	0	0.02	0.01	0	
	0.02	0.96	0.01	0.01	0	0	
	0.02	0.01	0.97	0	0	0	
	0.01	0.02	0	0.97	0	0	
	0.04	0.01	0	0	0.95	0	
	0.01	0	0.1	0.02	0	0.96	

(a)



(b)

Fig. 8 (a) Confusion matrix, and (b) ROC analysis.

According to Figure 8, the sample AK is misjudged as SK. Based on the clinical analysis, both SK and AK have

similar characteristics, which is the main reason for this misjudgement. The identification of SK and AK is the reason for local keratoses, flat papules, and brow rashes. In addition to this characteristic, the samples are misjudged because a greater number of AK images are presented in the database.

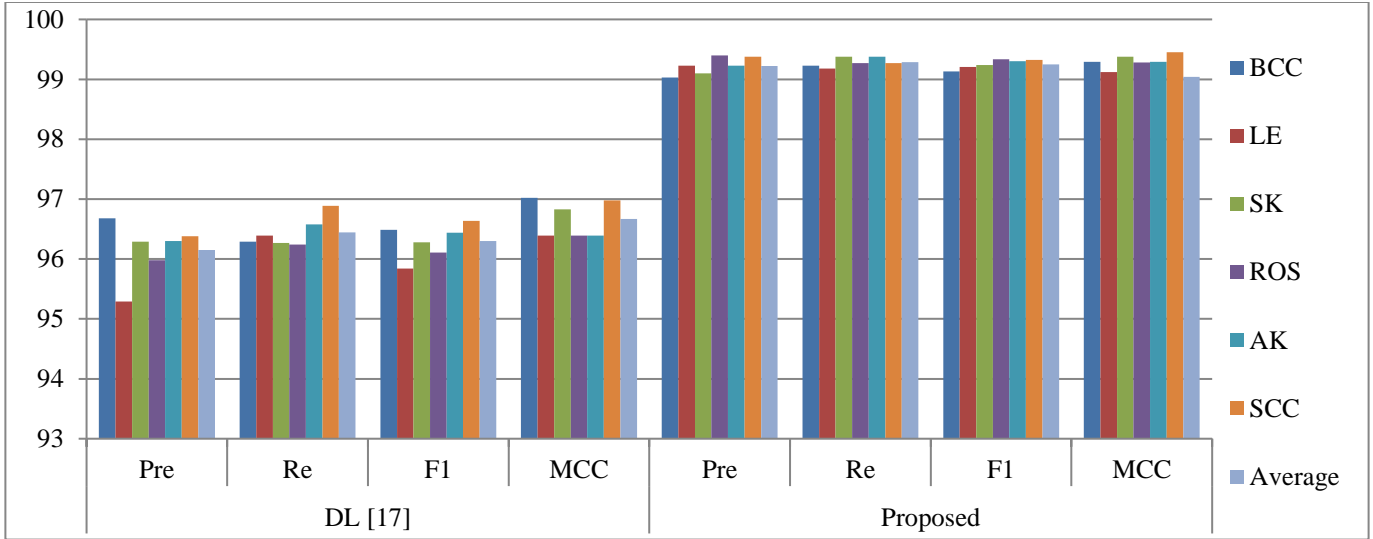
The confusion matrix clearly states that the introduced method eliminates the false classification while classifying the skin disease. Further, the excellence of the system is evaluated using Precision (pre), Recall (re), F1-score, and Matthew Correlation Coefficient (MCC) metrics.

Table 6 clearly shows that the optimized deep learning network introduced achieves a high accuracy of 99.25% while classifying different skin diseases. Thus, the issues related to obtaining highly accurate results are resolved in this research work. The introduced system combines the convolution $y_k = f(w_k * x)$ and pooling process $y_{kij} = \max_{\{p,q\} \in R_{ij}} x_{kpq}$ which helps to compute the features in the skin image with minimum complexity.

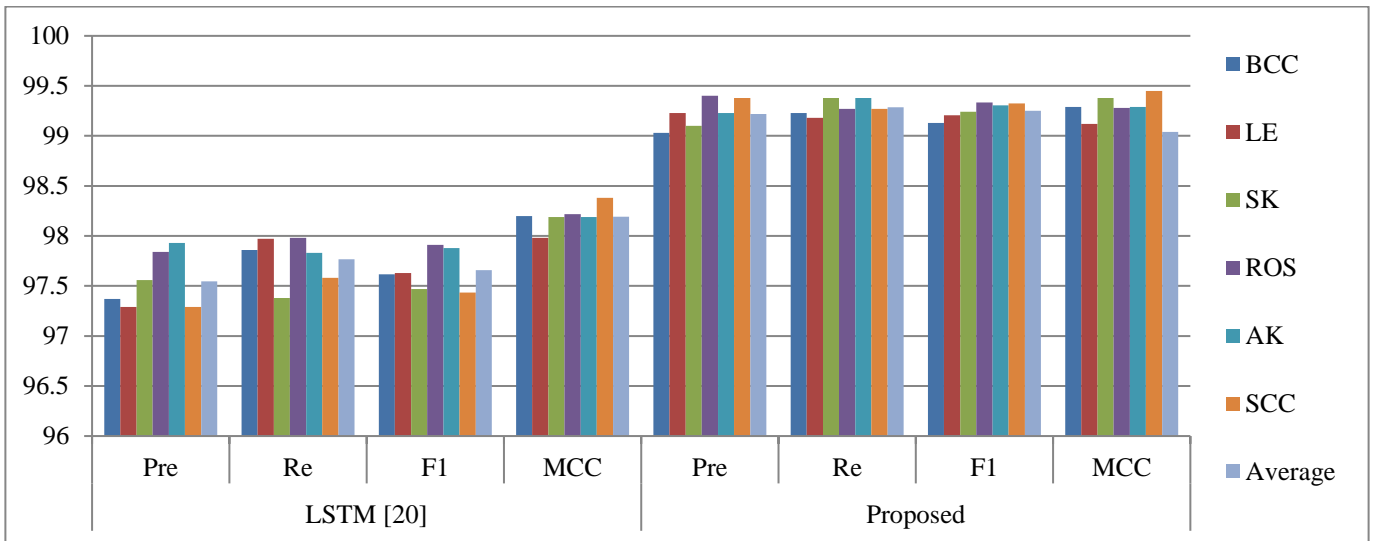
Furthermore, the feature map was successfully generated by inspecting each pixel in the image. In addition, the algorithm generates the training model before performing the classification model. The training process derives the patterns from the input image, which consists of several skin disease features. These features are more useful for classifying the testing images. From Figure 9, it is clearly stated that the introduced approach attains 99.04% of the MCC value while categorizing the various skin diseases from the face skin images. Effective weight updating, training, learning, and adaptive optimization techniques improve the overall skin disease identification process.

Table 6. Classification efficiency

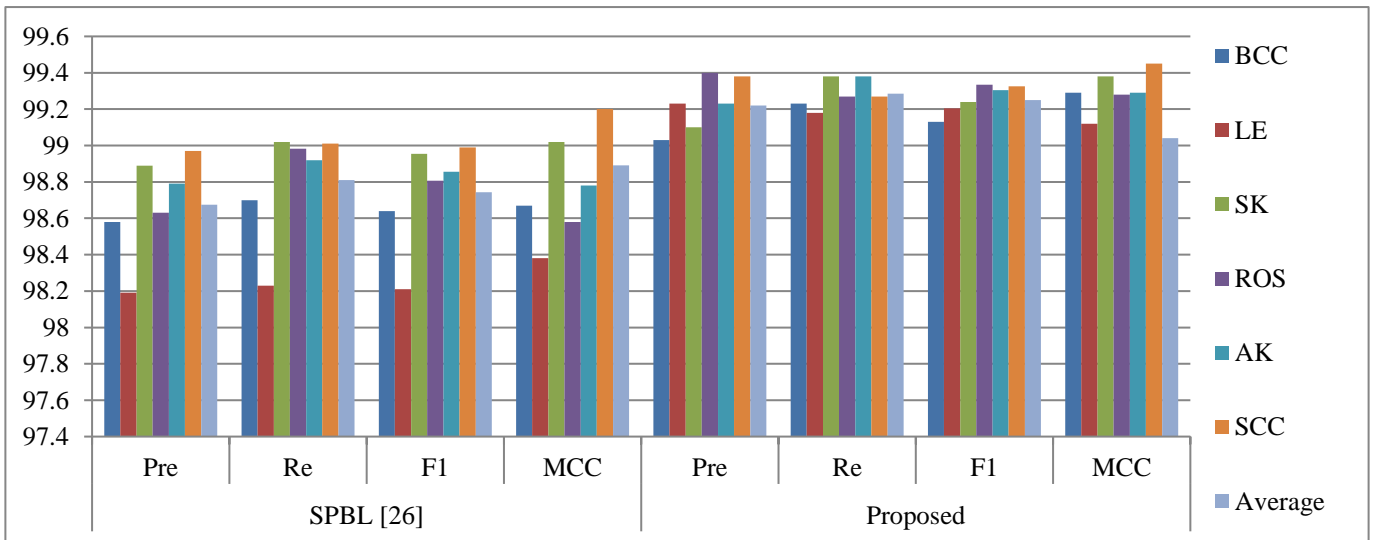
Method	Metric	BCC	LE	SK	ROS	AK	SCC	Average
DL [17]	Pre	96.68	95.29	96.29	95.98	96.3	96.38	96.1533
	Re	96.29	96.39	96.27	96.24	96.58	96.89	96.4433
	F1	96.485	95.84	96.28	96.11	96.44	96.635	96.2983
	MCC	97.02	96.389	96.83	96.39	96.39	96.98	96.6665
LSTM [20]	Pre	97.37	97.29	97.56	97.84	97.93	97.29	97.5467
	Re	97.86	97.97	97.38	97.98	97.83	97.58	97.7667
	F1	97.615	97.63	97.47	97.91	97.88	97.435	97.6567
	MCC	98.2	97.98	98.19	98.217	98.19	98.38	98.1928
SPBL [26]	Pre	98.58	98.19	98.89	98.63	98.79	98.97	98.675
	Re	98.7	98.23	99.02	98.982	98.92	99.01	98.8103
	F1	98.64	98.21	98.955	98.806	98.855	98.99	98.7427
	MCC	98.67	98.38	99.02	98.58	98.78	99.2	98.8917
Proposed	Pre	99.03	99.23	99.1	99.4	99.23	99.38	99.22
	Re	99.23	99.18	99.38	99.27	99.38	99.27	99.285
	F1	99.13	99.205	99.24	99.335	99.305	99.325	99.25
	MCC	99.29	99.12	99.38	99.28	99.29	99.45	99.04



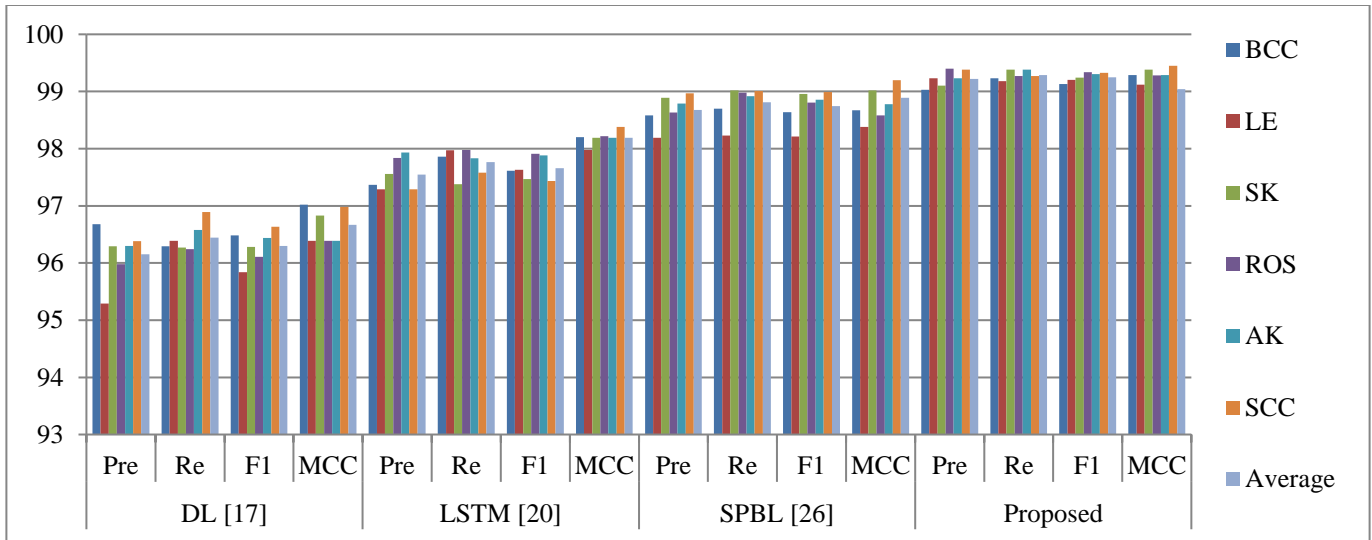
(a) DL [17] Vs Proposed system



(b) LSTM [20] Vs Proposed system



(c) SPBL [26] Vs Proposed system



(d) Overall performance
Fig. 9 Classification efficiency analysis

5. Conclusion

This research uses a median filtering method to process skin images obtained from Xiangya-Derma, China's largest clinical image database. The derived median value was utilized to remove the noise in the image but with the ability to make fine-grained distinctions at the edges of the image. Then, a convolution layer is used to segment the affected region. This process decreases computation complexity and increases skin disease classification accuracy. Various

texture- and colour-specific features are extracted from the segmented area and passed to a classifier to be analyzed. Computation complexity and overall skin disease classification are increased with an approach of using layering that merges convolution and pooling. The system mentioned here, developed with Python, is 99.04% sure of detecting skin diseases. Over time, the system will improve due to an improved feature selection process and due to optimizations, that will be enforced.

Reference

- [1] Kyungsu Lee et al., "Multi-Task and Few-Shot Learning-Based Fully Automatic Deep Learning Platform for Mobile Diagnosis of Skin Diseases," *IEEE Journal of Biomedical and Health Informatics*, vol. 27, no. 1, pp. 176-187, 2023. [CrossRef] [Google Scholar] [Publisher Link]
- [2] S. Gopalakrishnan, Abishek B. Ebenezer, and A. Vijayalakshmi, "An Erythematous Squamous Disease (ESD) Detection Using DBN Technique," *2022 International Conference on Communication, Computing and Internet of Things (IC3IoT)*, Chennai, India, pp. 1-4, 2022. [CrossRef] [Google Scholar] [Publisher Link]
- [3] Guanghui Yue et al., "Toward Multicenter Skin Lesion Classification Using Deep Neural Network with Adaptively Weighted Balance Loss," *IEEE Transactions on Medical Imaging*, vol. 42, no. 1, pp. 119-131, 2023. [CrossRef] [Google Scholar] [Publisher Link]
- [4] SajaSalim Mohammed, and Jamal Mustafa Al-Tuwaijari, "Skin Disease Classification System Based on Machine Learning Technique: A Survey," *IOP Conference Series: Materials Science and Engineering: 2nd International Scientific Conference of Engineering Sciences*, Diyala, Iraq, vol. 1076, no. 1, pp. 1-13, 2021. [CrossRef] [Google Scholar] [Publisher Link]
- [5] Bronwyn Shirley et al., "Radiation Therapy in the Adjuvant Treatment of Hyperkeratotic Palmoplantar Psoriasis: A Case Study," *Journal of Medical Radiation Sciences*, vol. 68, no. 3, pp. 326-331, 2021. [CrossRef] [Google Scholar] [Publisher Link]
- [6] Caihe Liao et al., "Combination Curettage and Modified Ala-Pdt for Multiple Basal Cell Carcinomas of the Face and Head," *Photodiagnosis and Photodynamic Therapy*, vol. 35, 2021. [CrossRef] [Google Scholar] [Publisher Link]
- [7] Gulsen Akoglu, et al., "Disease Severity and Poor Mental Health are the Main Predictors of Stigmatization in Patients with Hidradenitis Suppurativa," *Dermatologic Therapy*, vol. 34, no. 3, 2021. [CrossRef] [Google Scholar] [Publisher Link]
- [8] Andre Esteva et al., "Deep Learning-Enabled Medical Computer Vision," *NPJ Digital Medicine*, vol. 4, no. 1, pp. 1-9, 2021. [CrossRef] [Google Scholar] [Publisher Link]
- [9] Shuwei Shen et al., "Low-Cost and High-Performance Data Augmentation for Deep-Learning-Based Skin Lesion Classification," *Arxiv*, pp. 1-8, 2021. [CrossRef] [Google Scholar] [Publisher Link]
- [10] Evgin Goceri, "Diagnosis of Skin Diseases in the Era of Deep Learning and Mobile Technology," *Computers in Biology and Medicine*, vol. 134, 2021. [CrossRef] [Google Scholar] [Publisher Link]

- [11] Adekanmi Adegun, and SerestinaViriri, “Deep Learning Techniques for Skin Lesion Analysis and Melanoma Cancer Detection: A Survey of State-Of-The-Art,” *Artificial Intelligence Review*, vol. 54, pp. 811-841, 2021. [[CrossRef](#)] [[Google Scholar](#)] [[Publisher Link](#)]
- [12] Melina Tziomaka, “*Classifying Melanoma Images with Ensembles of Deep Convolutional Neural Networks*,” Master’s Thesis, University of Piraeus, 2021. [[Google Scholar](#)]
- [13] Gabriela Ribeiro de Araújo et al., “Leiomyoma and Leiomyosarcoma (Primary and Metastatic) Of the Oral and Maxillofacial Region: A Clinicopathological and Immunohistochemical Study of 27 Cases,” *Head and Neck Pathology*, vol. 16, pp. 294-303, 2021. [[CrossRef](#)] [[Google Scholar](#)] [[Publisher Link](#)]
- [14] Peng Yao et al., “Single Model Deep Learning on Imbalanced Small Datasets for Skin Lesion Classification,” *Arxiv*, pp. 1-13, 2021. [[CrossRef](#)] [[Google Scholar](#)] [[Publisher Link](#)]
- [15] Rania Ramadan, and Saleh Aly, “CU-Net: A New Improved Multi-Input Color U-Net Model for Skin Lesion Semantic Segmentation,” *IEEE Access*, vol. 10, pp. 15539-15564, 2022. [[CrossRef](#)] [[Google Scholar](#)] [[Publisher Link](#)]
- [16] Fengying Xie et al., “Skin Lesion Segmentation Using High-Resolution Convolutional Neural Network,” *Computer Methods and Programs in Biomedicine*, vol. 186, 2020. [[CrossRef](#)] [[Google Scholar](#)] [[Publisher Link](#)]
- [17] Jianxiao Bian et al., “Skin Lesion Classification by Multi-View Filtered Transfer Learning,” *IEEE Access*, vol. 9, pp. 66052-66061, 2021. [[CrossRef](#)] [[Google Scholar](#)] [[Publisher Link](#)]
- [18] SeungSeog Han et al., “Classification of the Clinical Images for Benign and Malignant Cutaneous Tumors Using a Deep Learning Algorithm,” *Journal of Investigative Dermatology*, vol. 138, no. 7, pp. 1529-1538, 2018. [[CrossRef](#)] [[Google Scholar](#)] [[Publisher Link](#)]
- [19] Li-sheng Wei, Quan Gan, and Tao Ji, “Skin Disease Recognition Method Based on Image Color and Texture Features,” *Computational and Mathematical Methods in Medicine*, vol. 2018, no. 1, pp. 1-10, 2018. [[CrossRef](#)] [[Google Scholar](#)] [[Publisher Link](#)]
- [20] Sourav Kumar Patnaik et al., “Automated Skin Disease Identification Using Deep Learning Algorithm,” *Biomedical and Pharmacology Journal*, vol. 11, no. 3, pp. 1429-1437, 2018. [[CrossRef](#)] [[Google Scholar](#)] [[Publisher Link](#)]
- [21] Parvathaneni Naga Srinivasu et al., “Classification of Skin Disease Using Deep Learning Neural Networks with Mobilenet V2 and LSTM,” *Sensors*, vol. 21, no. 8, pp. 1-27, 2021. [[CrossRef](#)] [[Google Scholar](#)] [[Publisher Link](#)]
- [22] Zhe Wu et al., “Studies on Different CNN Algorithms for Face Skin Disease Classification Based on Clinical Images,” *IEEE Access*, vol. 7, pp. 66505-66511, 2019. [[CrossRef](#)] [[Google Scholar](#)] [[Publisher Link](#)]
- [23] Tri-Cong Pham et al., “Improving Skin-Disease Classification Based on Customized Loss Function Combined With Balanced Mini-Batch Logic and Real-Time Image Augmentation,” *IEEE Access*, vol. 8, pp. 150725-150737, 2020. [[CrossRef](#)] [[Google Scholar](#)] [[Publisher Link](#)]
- [24] Belal Ahmad et al., “Discriminative Feature Learning for Skin Disease Classification Using Deep Convolutional Neural Network,” *IEEE Access*, vol. 8, pp. 39025-39033, 2020. [[CrossRef](#)] [[Google Scholar](#)] [[Publisher Link](#)]
- [25] Yanyang Gu et al., “Progressive Transfer Learning and Adversarial Domain Adaptation for Cross-Domain Skin Disease Classification,” *IEEE Journal of Biomedical and Health Informatics*, vol. 24, no. 5, pp. 1379-1393, 2020. [[CrossRef](#)] [[Google Scholar](#)] [[Publisher Link](#)]
- [26] Peng Tang et al., “GP-CNN-DTEL: Global-Part CNN Model With Data-Transformed Ensemble Learning for Skin Lesion Classification,” *IEEE Journal of Biomedical and Health Informatics*, vol. 24, no. 10, pp. 2870-2882, 2020. [[CrossRef](#)] [[Google Scholar](#)] [[Publisher Link](#)]
- [27] Jufeng Yang et al., “Self-Paced Balance Learning for Clinical Skin Disease Recognition,” *IEEE Transactions on Neural Networks and Learning Systems*, vol. 31, no. 8, pp. 2832-2846, 2020. [[CrossRef](#)] [[Google Scholar](#)] [[Publisher Link](#)]
- [28] Anuj Kumar Singh et al., “A Proportional Sentiment Analysis of MOOCs Course Reviews Using Supervised Learning Algorithms,” *International Information and Engineering Technology Association*, vol. 26, no. 5, pp. 501-506, 2021. [[CrossRef](#)] [[Google Scholar](#)] [[Publisher Link](#)]
- [29] Shashi Bhushan et al., “A Novel Approach to Face Pattern Analysis,” *Electronics*, vol. 11, no. 3, pp. 1-14, 2022. [[CrossRef](#)] [[Google Scholar](#)] [[Publisher Link](#)]
- [30] Shashi Bhushan et al., “An Experimental Analysis of Various Machine Learning Algorithms for Hand Gesture Recognition,” *Electronics*, vol. 11, no. 6, pp. 1-15, 2022. [[CrossRef](#)] [[Google Scholar](#)] [[Publisher Link](#)]
- [31] Vimal K. Shrivastava et al., “Reliability Analysis of Psoriasis Decision Support System in Principal Component Analysis Framework,” *Data and Knowledge Engineering*, vol. 106, pp. 1-17, 2016. [[CrossRef](#)] [[Google Scholar](#)] [[Publisher Link](#)]
- [32] Vimal K. Shrivastava et al., “Computer-Aided Diagnosis of Psoriasis Skin Images with HOS, Texture and Color Features: A First Comparative Study of its Kind,” *Computer Methods and Programs in Biomedicine*, vol. 126, pp. 98-109, 2016. [[CrossRef](#)] [[Google Scholar](#)] [[Publisher Link](#)]
- [33] Fujia Ren, Chenhui Yang, and Y.A. Nanekaran, “MRI-Based Model for MCI Conversion Using Deep Zero-Shot Transfer Learning,” *The Journal of Supercomputing*, vol. 79, pp. 1182-1200, 2023. [[CrossRef](#)] [[Google Scholar](#)] [[Publisher Link](#)]
- [34] Y.A. Nanekaran et al., “Analysis and Comparison of Machine Learning Classifiers and Deep Neural Networks Techniques for Recognition of Farsi Handwritten Digits,” *The Journal of Supercomputing*, vol. 77, pp. 3193-3222, 2021. [[CrossRef](#)] [[Google Scholar](#)] [[Publisher Link](#)]

- [35] Md. Kowsher et al., "LSTM-ANN and BiLSTM-ANN: Hybrid Deep Learning Models for Enhanced Classification Accuracy," *Procedia Computer Science*, vol. 193, pp. 131-140, 2021. [[CrossRef](#)] [[Google Scholar](#)] [[Publisher Link](#)]
- [36] Y.A. Nanekaran et al., "A Pragmatic Convolutional Bagging Ensemble Learning for Recognition of Farsi Handwritten Digits," *The Journal of Supercomputing*, vol. 77, pp. 13474-13493, 2021. [[CrossRef](#)] [[Google Scholar](#)] [[Publisher Link](#)]